Electronic Supplementary Material
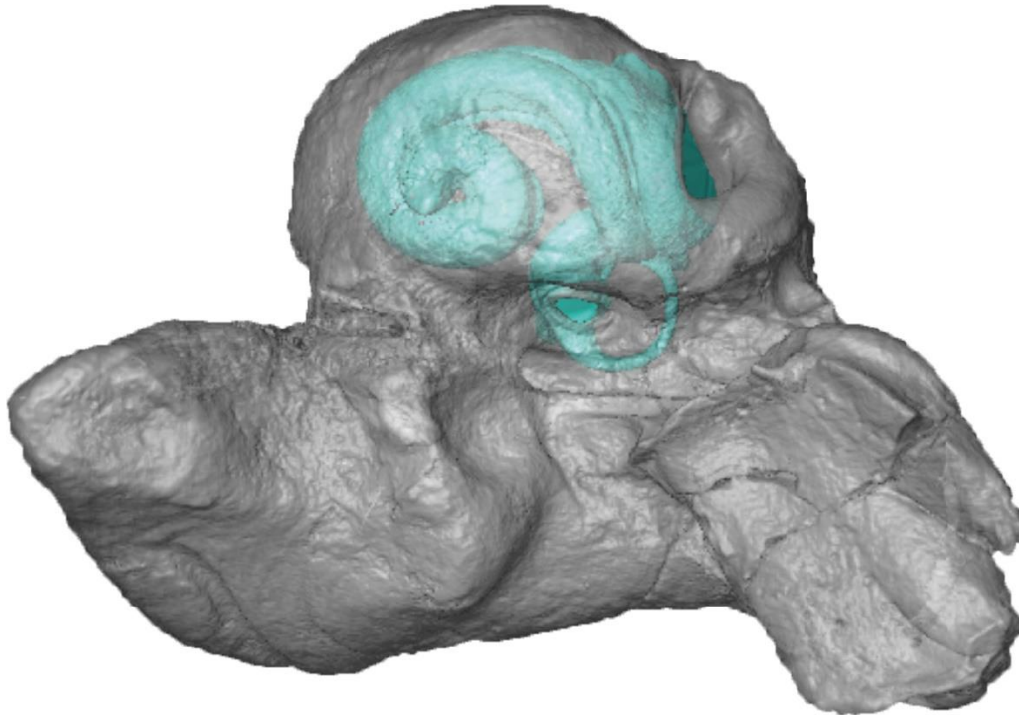
Example of periotic with inner ear reconstruction

Fig. S1. *Aondelphis talen* periotic in ventral view (transparent) with its corresponding inner ear reconstruction (blue), in order to exemplify how both structures are related.

3D Geometric morphometric analyses supplementary results

When analyzing P+O_Coch dataset, the morphospace occupied by the Platanistoidea includes Delphinida, Physeteroidea, Ziphioidea and stem Odontoceti (Fig. S2). Basilosauridae (*Zygorhiza* sp.) is on the extreme positive side of PC1. Along PC1, shape variation includes width of the basal and apical turns and area of the fenestra vestibuli, whilst in PC2 the tightness and height of the cochlea. The phylomorphospace (Fig. S3) shows a similar pattern than the complete inner ear dataset, but with a reduced occupation of the morphospace (i.e. less morphological variation is present when analyzing the cochlea alone). On the other hand, the CVA analysis (excluding Basilosauridae) clearly differentiates Physeteroidea + Ziphioidea and stem Odontoceti on the one hand, and Platanistoidea and Delphinida on the other hand. Here

again, the morphospace occupied in the first two CV axes by Platanistoidea is the largest (Fig. S4).

For the P_Coch dataset, again the PCA does not clearly differentiate between the different families (Fig. S5). PC1 and PC2 account for 66% of the total variation. PC1 includes a wider cochlea and basal turn, whilst PC2 shows variation in the tightness of the cochlea and position of the vestibular aqueduct. Both Platanistidae and Waipatiidae have the widest morphospaces, with a clear overlap in PC1 between *Notocetus* and *A. talen* with the waipatiids. The phylomorphospace (Fig. S6) shows that the longest branches (and therefore, more different morphologies) are present in *Z. crassangulum, W. maerewhenua, S. calvertensis, A. tokarahi* and *P. gangetica*. As for the CVA (Fig. S7), it more clearly separates the different families, with an overlap between Waipatiidae, stem Odontoceti and Platanistidae on CV1. On the other hand, stem Platanistoidea (*Notocetus* and *A. talen*) are clearly separated from the remaining families.
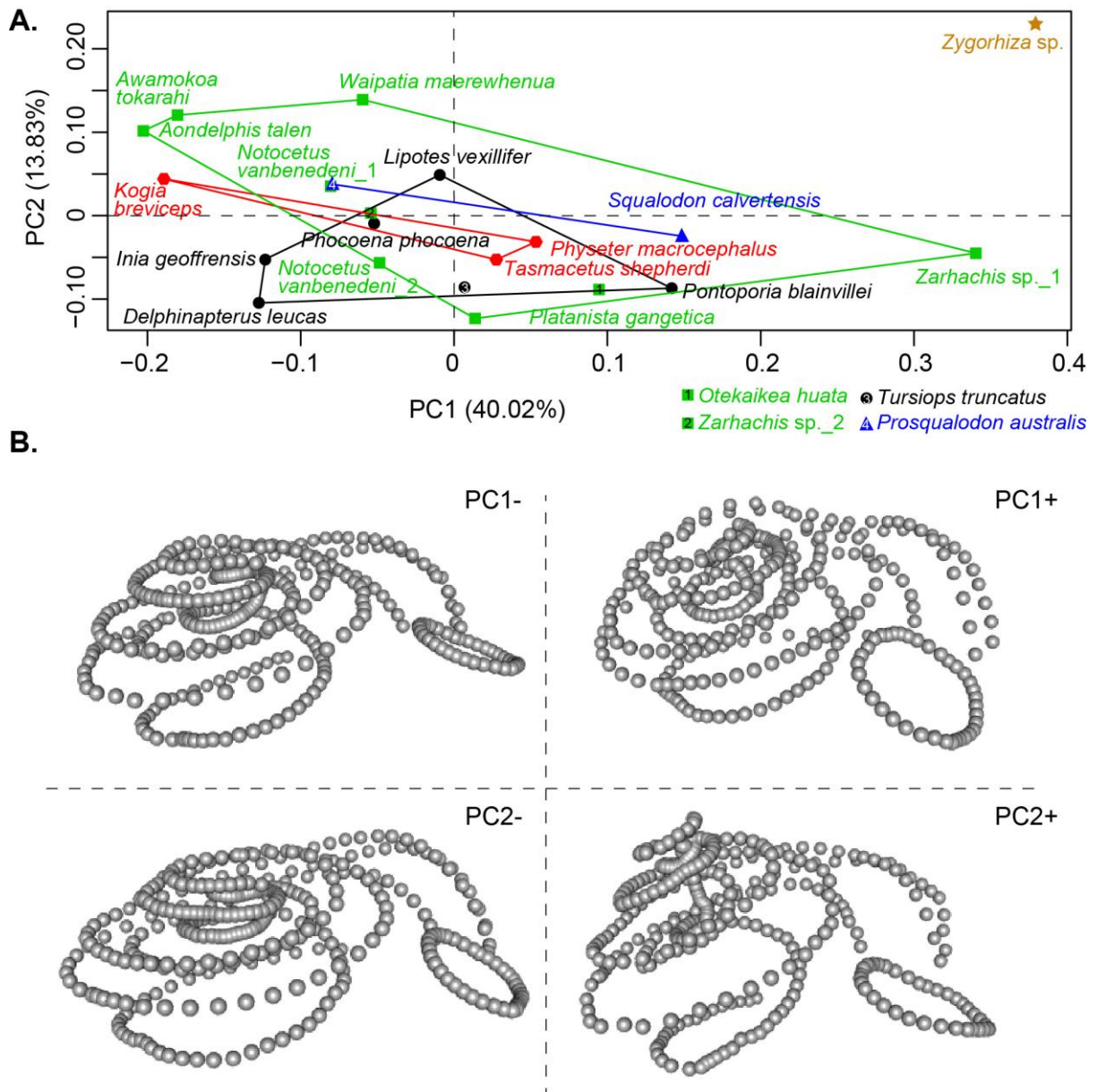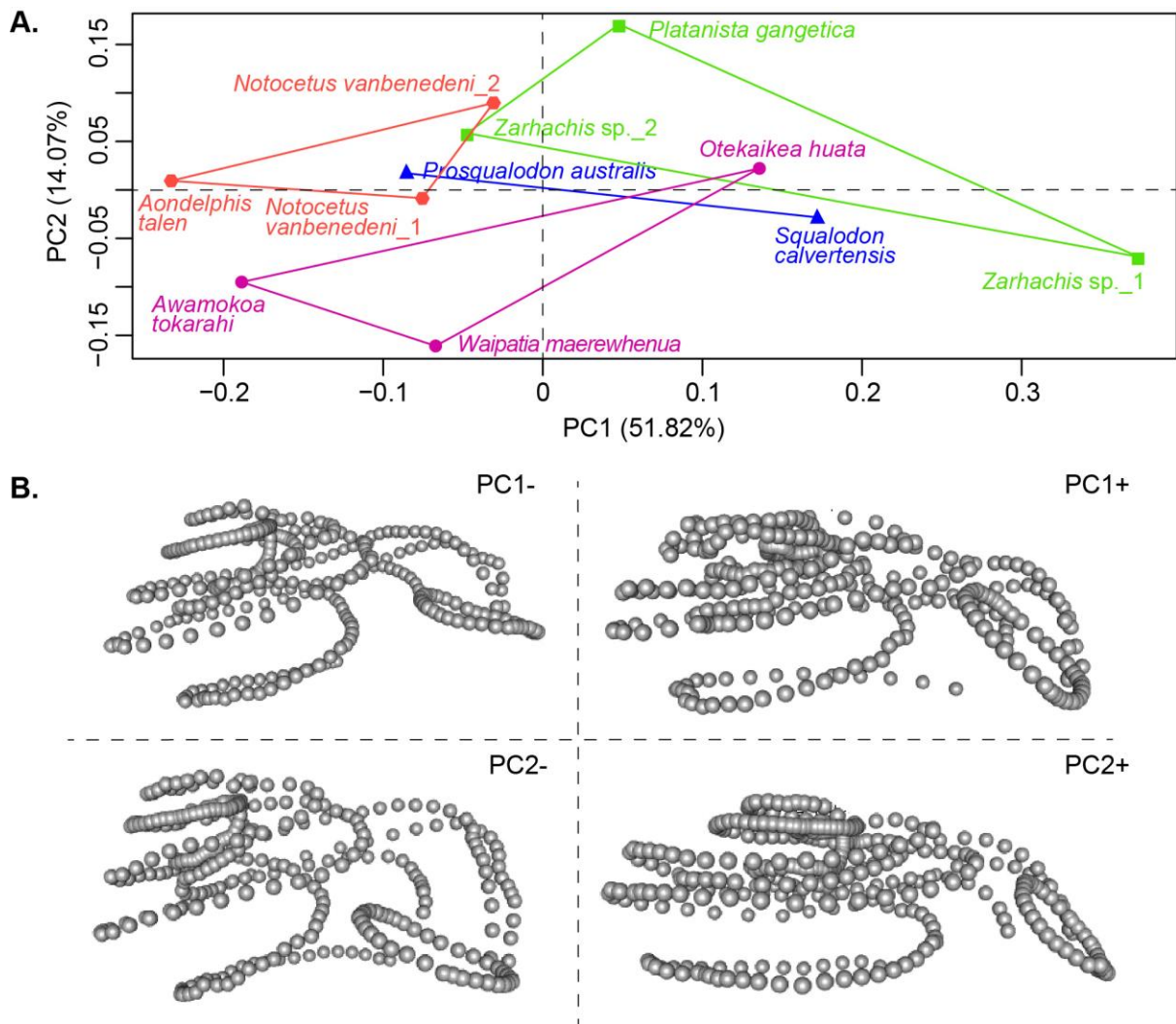
Fig. S2. PCA plot of the cochlea (P+O_Coch) dataset of all Odontoceti species included in our study. Color legend: red polygon, Physeteridae + Ziphiidae; green square, Platanistoidea; blue triangle, stem Odontoceti; black circle, Delphinida; brown, Basilosauridae. Below are the extreme configurations for each PC axis.
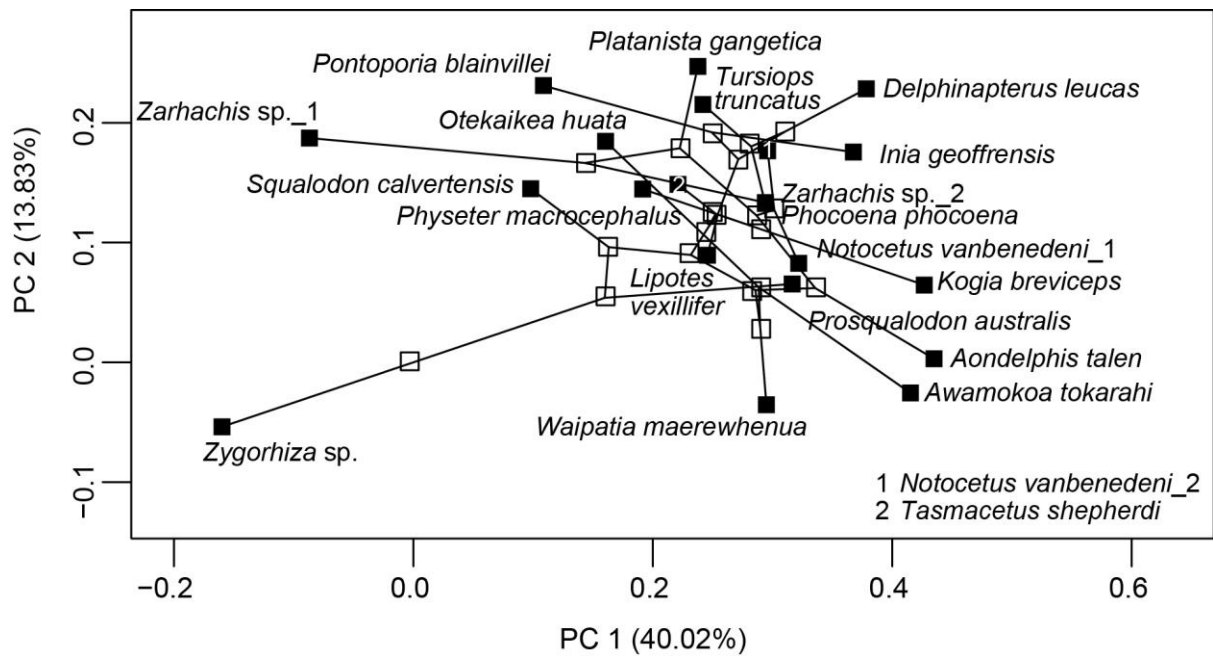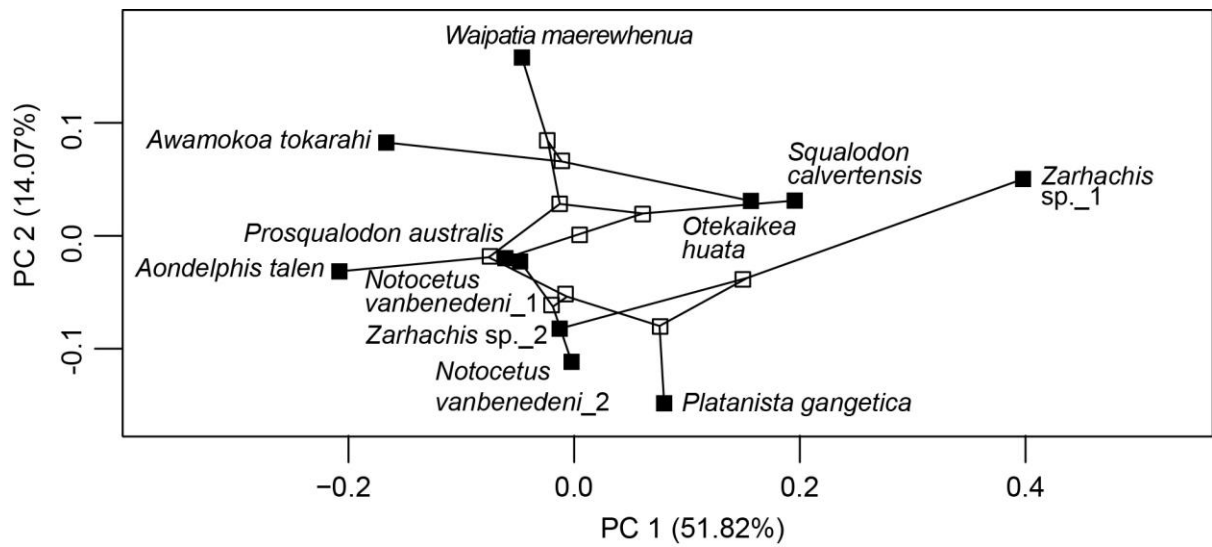
Fig S3. Phylomorphospace plot of the first two PC of the cochlea (P+O_Coch) dataset of Odontoceti species included in our study (excluding Basilosauridae). Black squares denote the position of each taxon, whilst unfilled squares represent the inferred position of the internal nodes.
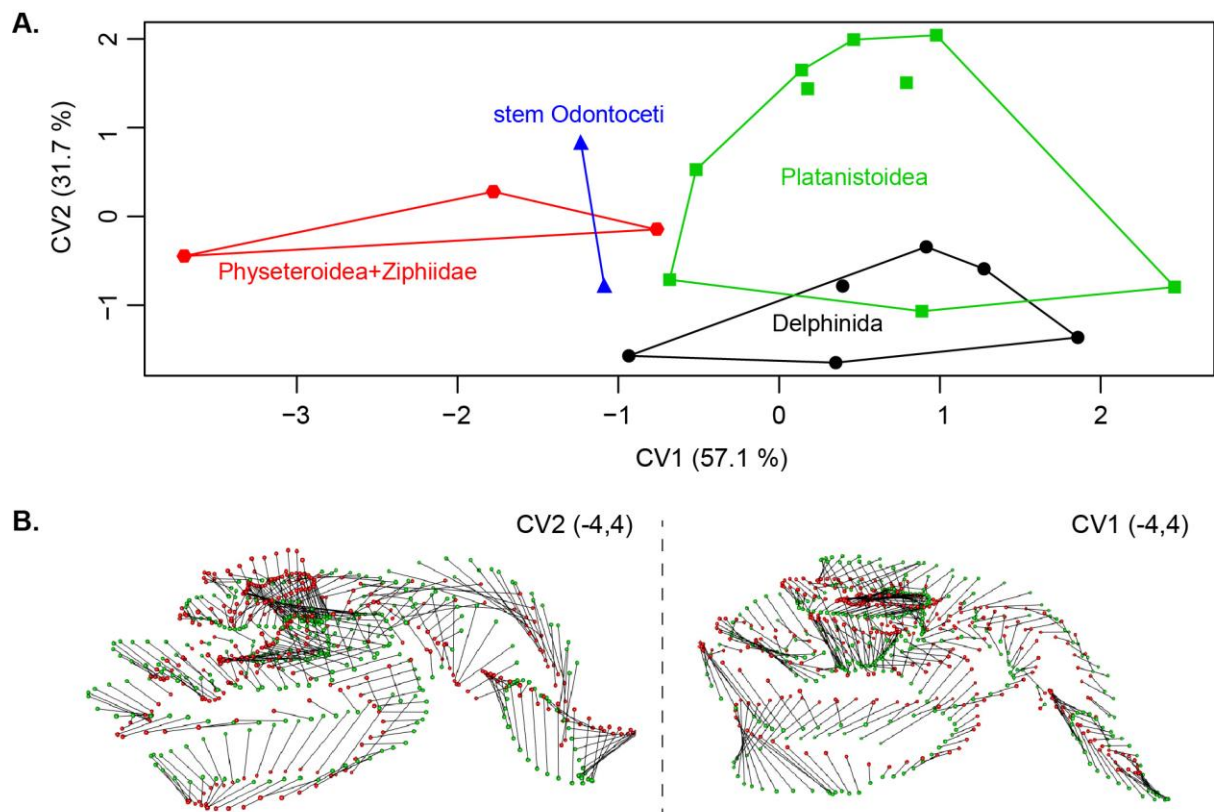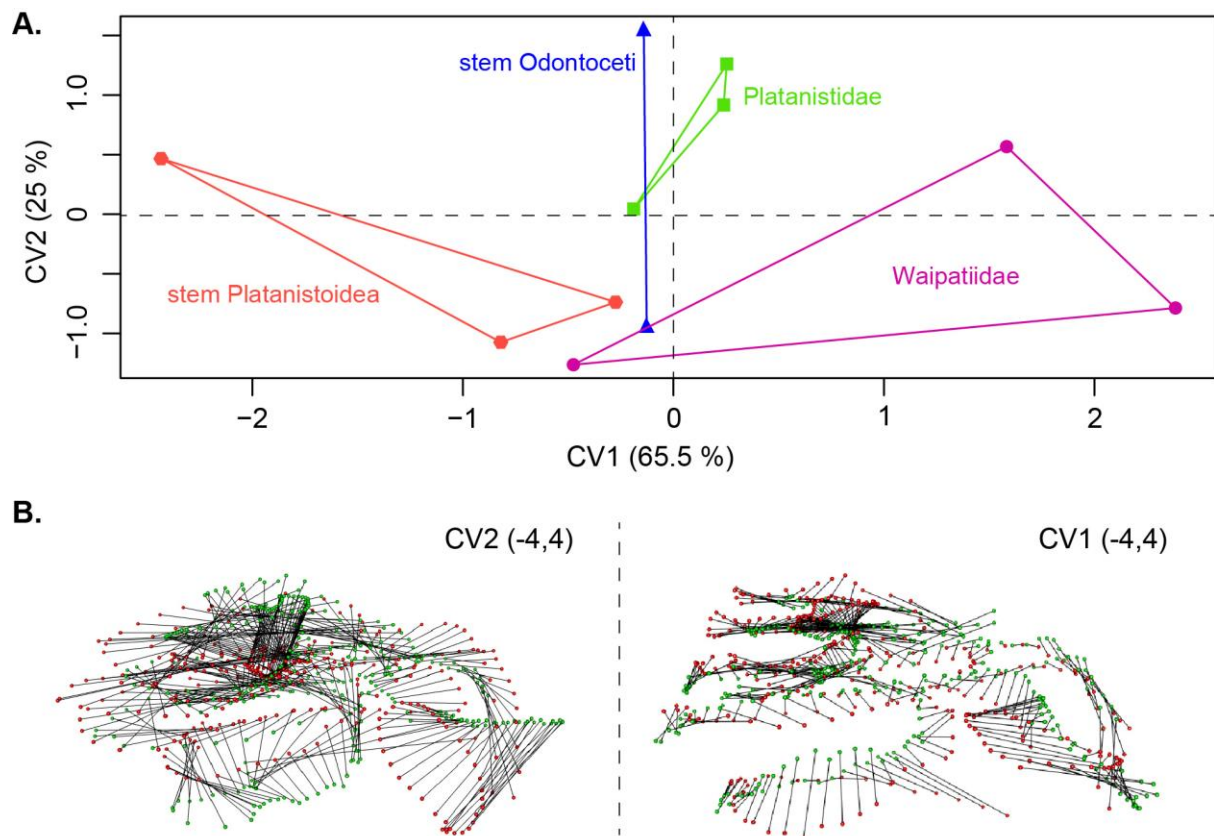
Fig S4. CVA plot of the cochlea (P+O_Coch) dataset of all Odontoceti species included in our study (except Basilosauridae, see Material and Methods for explanation). Color legend: green square, Platanistoidea; blue triangle, stem Odontoceti; red polygon, Physeteroidea + Ziphiidae; black circle, Delphinida. Below are the extreme configurations for each CV axis, red dots represent the positive extreme and green dots the negative extreme configurations.

Fig. S5. PCA plot of the cochlea (P_Coch) dataset of Platanistoidea species only included in our study. References: red polygon, stem Platanistoidea; violet circle, Waipatiidae; green square, Platanistidae; blue triangle, stem Odontoceti. Below are the extreme configurations for each PC axis.

Fig S6. Phylomorphospace plot of the first two PC of the cochlea (P_Coch) dataset of of Platanistoidea species included in our study. Black squares denote the position of each taxon, whilst unfilled squares represent the inferred position of the internal nodes.

Fig S7. CVA plot of the cochlea (P_Coch) dataset of Platanistoidea species included in our study. Color legend: red polygon, stem Platanistoidea; violet circle, Waipatiidae; green square, Platanistidae; blue triangle, stem Odontoceti. Species included in each group are defined following Viglino et al. (2018a,b). Below are the extreme configurations for each CV axis, red dots represent the positive extreme and green dots the negative extreme configurations.